Applied Catalysis A: General 377 (2010) 35–41

Contents lists available at ScienceDirect

Applied Catalysis A: General

journal homepage: www.elsevier.com/locate/apcata

Supported indium oxide as novel efficient catalysts for dehydrogenation of propane with carbon dioxide

Miao Chen, Jie Xu, Yong-Mei Liu, Yong Cao *, He-Yong He, Ji-Hua Zhuang *

Shanghai Key Laboratory of Molecular Catalysis and Innovative Materials, Department of Chemistry, Fudan University, No. 220#, Handan Road, Shanghai 200433, PR China

ARTICLE INFO

Article history:
Received 18 August 2009
Received in revised form 23 December 2009
Accepted 9 January 2010
Available online 18 January 2010

Keywords:
Indium oxide
Dehydrogenation
Propane
Propylene
Carbon dioxide

ABSTRACT

In_2O_3–MO_x binary mixed metal oxide catalysts (M: Al, Zn, Zr, Ti, Fe, Mg, Si, and Ce) prepared by a coprecipitation or sol–gel method have been tested for the dehydrogenation of propane to propylene in the presence of carbon dioxide. Several techniques including N_2 adsorption/desorption, X-ray diffraction, H_2-temperature-programmed reduction and X-ray photoelectron spectroscopy were applied to characterize the physicochemical properties of the as-synthesized materials. Catalytic tests showed that all In-containing samples were active in the CO_2-promoted dehydrogenation of propane with good propylene selectivity. Among the In_2O_3–MO_x catalysts tested, the In_2O_3–Al_2O_3 sample containing a 20 mol% indium content showed the highest dehydrogenation activity with superior long-term stability. The specific interaction between In_2O_3 and Al_2O_3 leading to a high component dispersion is suggested to play a key role in regulating the redox and structural properties of surface indium species, which makes the In_2O_3–Al_2O_3 composite highly active and stable for the reaction.

1. Introduction

The catalytic dehydrogenation of alkanes is of the considerable industrial importance, for it represents a route that economically upgrades low-cost saturated hydrocarbons into the more expensive alkenes [1]. In this context, much effort has been dedicated to the dehydrogenation (DH) of propane to propylene [2–4] given the rapidly growing demand for propylene in the production of propylene oxide, acrylonitrile, and polypropylene. However, the DH of propane has inherent drawbacks: thermodynamic limitations for propane conversion, high energy requirements due to endothermic reaction and limited catalytic stability owing to coke formation [5,6]. As an alternative to DH, oxidative dehydrogenation (ODH) of propane by molecular oxygen offers the possibility of being an energy-saving process for propylene production [7–10]. Nevertheless, the ODH process suffers from a significant loss of propylene selectivity due to formation of total oxidation products and has a number of safety issues.

Recently, the use of CO_2 as a mild oxidant to activate the short chain alkanes has emerged as new promising technology for the development of safer, more economical and environmentally friendly propane dehydrogenation process [11–13]. It has been shown that in this new process propylene can be obtained with a higher yield than in the commercial one. The promotion effect of the presence of CO_2 in the reaction stream has been attributed to an increase of the dehydrogenation efficiency via a direct surface redox mechanism in which the catalyst undergoes reduction (by propane) and reoxidation (by CO_2) cycles [14–16] or a more complex reaction pathway involving a simple dehydrogenation followed by the reverse water gas shift (RWGS) reaction [17–19]. In the latter case CO_2 removes hydrogen from the reaction system and releases the thermodynamic restrictions. It has been demonstrated that in many catalyst systems propylene formation is promoted by both presented mechanisms [20]. Moreover, in the dehydrogenation process CO_2 can act as a diluent [19,21,22], it delivers the required heat and reduces coking of catalyst by the coke gasification.

Among all the studied catalysts, the supported gallium oxide-based materials have been documented as the most promising ones due to their high catalytic efficiency [19,23,24]. One critical limitation associated with the conventional Ga_2O_3-catalyzed propane DH process, however, is the drastic deactivation during a few hours on-stream [19,25,26]. Very recently, we have demonstrated that Ga_2O_3–Al_2O_3 mixed oxides are highly active and stable catalysts for propane dehydrogenation in the presence of CO_2 [17,18]. The superior performance of the Ga_2O_3–Al_2O_3-system has been attributed to the formation of gallia-alumina solid solution between Ga_2O_3 and Al_2O_3 [18], which can allow the favorable creation of a high abundance of surface gallium sites with weak Lewis acidity. However, the development of new improved catalytic system that exhibits desirable stability and activity still remains a major challenge.

* Corresponding authors. Tel.: +86 21 55665287; fax: +86 21 65643774.
E-mail addresses: yongcao@fudan.edu.cn (Y. Cao), jihuaz@fudan.edu.cn (J.-H. Zhuang).

0926-860X/$ – see front matter © 2010 Elsevier B.V. All rights reserved.
doi:10.1016/j.apcata.2010.01.011

Supported In_2O_3-based materials have received limited attention as dehydrogenation catalysts, despite their excellent performance to activate hydrocarbon species in the selective catalytic reduction (de-NO_x) reactions [27–31]. On the other hand, it is also well established that Ga-containing catalysts have shown to exhibit high activity and selectivity in the de-NO_x reactions [32–34]. In view of the catalytic similarities between Ga_2O_3- and In_2O_3-based systems, we envisioned that it would be of interest to explore the activity of supported indium oxide for propane dehydrogenation to propylene with CO_2. In the present study, we show that In_2O_3–Al_2O_3 is one of the most effective materials for propane dehydrogenation in the presence of CO_2. The catalytic stability and deactivation behavior of the In_2O_3-based catalysts were also examined.

2. Experimental

2.1. Catalyst preparation

Various In_2O_3–MO_x mixed oxide catalysts (M: Al, Zn, Zr, Ti, Fe, Mg, Si, and Ce) with In molar percentage of 20% were prepared via two different synthetic approaches, i.e., coprecipitation and sol–gel method. For mixed oxides with M = Al, Zr, Fe, Mg, Zn, Ce as well as the simple oxide of In_2O_3 and Ga_2O_3, the coprecipitation method was employed. In a typical synthesis, concentrated aqueous ammonia and ethanol (50:50 in volume) was added dropwise to the ethanol solution of indium nitrate (Aldrich, 99.99%) and the corresponding metal nitrate (Fluka, 99.9%) until no more precipitation occurred. The precipitates was recovered by filtration, washed thoroughly and dried in air at 373 K for 12 h, followed by calcination at 873 K in air for 6 h.

When $TiCl_4$ or $Si(OEt)_4$ (Aldrich, 99.99%) were used as the starting materials, sol–gel method was employed to prepare the In_2O_3–MO_x composite materials. Typically, indium nitrate and $TiCl_4$ were dissolved simultaneously in an alcoholic solution under vigorous stirring at room temperature. The pH value was adjusted by adding NaOH dropwise until pH 10 was reached. After aging for 24 h, the gel was filtrated and thoroughly washed by 3 L distilled water. The drying and calcination treatment was the same as that of the coprecipitation method. The final catalyst is denoted as In–M-*n* hereinafter where M denotes the second metal, *n* represents the mole percentage of In_2O_3.

2.2. Catalyst characterization

The BET specific surface areas of the samples were determined by adsorption–desorption of nitrogen at liquid nitrogen temperature, using a Micromeritics TriStar 3000 equipment. The X-ray photoelectron spectroscopy (XPS) data of the samples were acquired using a PerkinElmer PHI 5000C spectrometer working in the constant analyzer energy mode with Mg Kα radiation as the excitation source. The carbonaceous C 1s line (284.6 eV) was used as the reference to calibrate the binding energies (BE). Thermal gravimetric analysis (TGA) was conducted on a PerkinElmer TGA-7 apparatus to determine the amount of coke deposited on the catalyst after the reaction. Twenty milligrams of sample was heated from room temperature to 873 K at a heating rate of 10 K min^{-1} in flowing air.

The X-ray powder diffraction (XRD) of the catalysts was carried out on a Germany Bruker D8Advance X-ray diffractometer using nickel filtered Cu Kα radiation (λ = 1.5418 Å) at 40 kV and 20 mA. Elemental analysis was performed using ion-coupled plasma (ICP) atomic emission spectroscopy on a Thermo Electron IRIS Intrepid II XSP spectrometer. Temperature-programmed reduction (TPR) results were obtained on a homemade apparatus loaded with 20 mg of catalyst. The air-pretreated samples were heated from room temperature to a final temperature of 1073 K at a rate of 5 K min^{-1} in an H_2/Ar stream (H_2/Ar molar ratio of 5/95 and a total flow of 40 mL min^{-1}). The H_2 consumption was monitored using a TCD detector.

2.3. Catalytic activity tests

Catalytic tests were performed in a fixed-bed microreactor at ambient pressure. The catalyst load was 200 mg, and it was activated at 873 K in N_2 for 2 h prior to the reaction. The feed gas contained 2.5 vol% propane, 10 vol% CO_2 and balancing nitrogen. The total flow rate of gas reactant was 10 mL min^{-1}. The feed and the reaction products were analyzed on-line by on-line gas chromatograph (Type GC-122, Shanghai). Permanent gases (CO and CO_2) and water (H_2O) were separated using a TDX-01 column connected to a TCD detector and other reaction products were analyzed employing a Porapak Q column connected to a FID detector. Blank runs show that under the experimental conditions used in this work the thermal dehydrogenation could be neglected.

3. Results

3.1. Dehydrogenation activity

The effect of the second metal oxide employed in the In_2O_3–MO_x binary mixed oxides (In_2O_3 mole content fixed at 20%) was tested in the dehydrogenation of propane with 10 kPa CO_2 used as weak oxidant under steady-state conditions at 873 K. In all cases, the major product formed in the reaction is propylene, and the minor products are ethane, ethylene, and methane. Fig. 1 compares the propylene yields on various mixed oxide catalysts. For the sake of comparison, the activity of bulk In_2O_3 is also included. While all In_2O_3–MO_x binary mixed oxides display an appreciable or pronounced activity for propylene formation, the simple oxide of bulk In_2O_3 demonstrated a very low activity. This poor activity is consistent with the inferior activity of indium oxide or other metal oxides as reported in the literature [24], indicating that the dispersion of In_2O_3 by a second metal oxide is indispensable for the genesis of catalytically active sites for alkane dehydrogenation. In_2O_3–Al_2O_3 afforded the highest yield of propylene (25.6%) amongst the various binary metal oxide catalysts. The order of the steady activity of binary metal oxides at the reaction temperature of 873 K was as follows: In–Al-20 > In–Zn-20 > In–Zr-20 > In–Ti-20 > In–Fe-20 > In–Mg-20 > In–Si-20 > In–Ce-20.

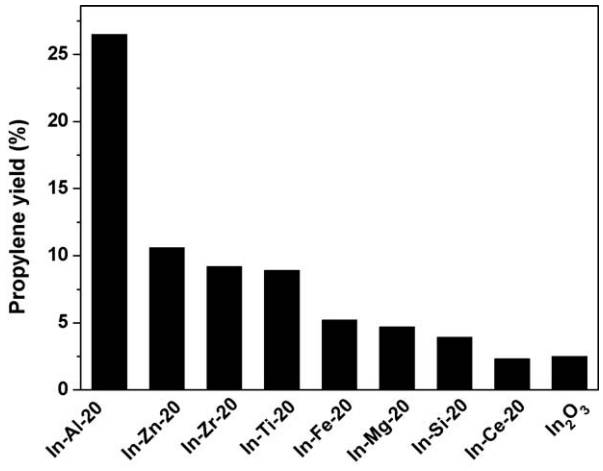

Fig. 1. Yield of propylene for various In–M–O mixed oxide with In_2O_3 molar percentage of 20% and In_2O_3 in the dehydrogenation of propane with CO_2. Reaction conditions: catalyst weight: 200 mg; P (C_3H_8) = 2.5 kPa; P (CO_2) = 10 kPa; P (N_2) = 87.5 kPa; reaction temperature: 873 K; total flow rate: 10 mL min^{-1}.

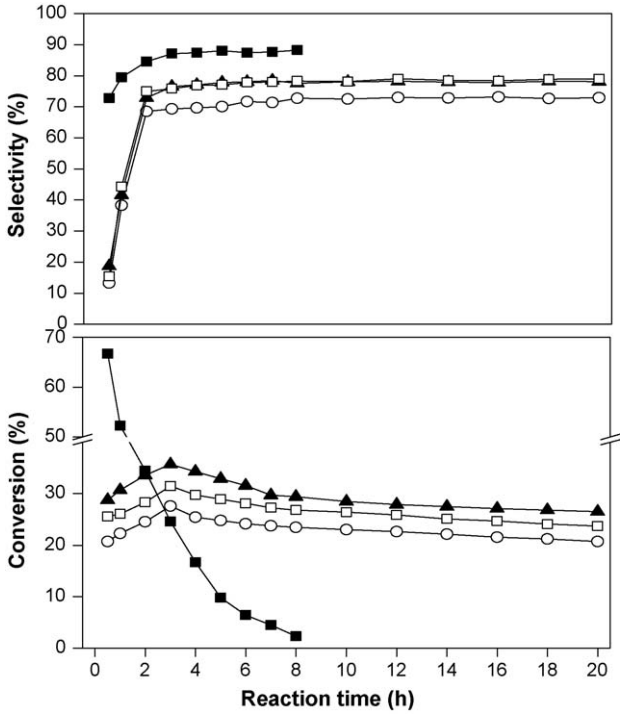

Fig. 2. Conversion of propane and selectivity to propylene as a function of time-on-stream for In_2O_3–Al_2O_3 mixed oxides. (□) In–Al-10; (▲) In–Al-20; (○) In–Al-40; and (■) β-Ga_2O_3. Reaction conditions––catalyst weight: 200 mg; $P(C_3H_8)$ = 2.5 kPa; $P(CO_2)$ = 10 kPa; $P(N_2)$ = 87.5 kPa; reaction temperature: 873 K; total flow rate: 10 mL min^{-1}.

The propylene selectivities in all the binary metal oxide catalysts were >75% in the dehydrogenation of propane in the presence of CO_2.

The conversion of propane over different compositions of In_2O_3–Al_2O_3 mixed oxide catalysts as a function of the reaction time has been depicted in Fig. 2. It is apparent that all samples exhibited a very low selectivity toward propylene formation in the initial stage of the reaction, suggesting that an induction period is required to develop the active site. The results, reported in Table 1, show that the In_2O_3–Al_2O_3 nanocomposites all led to a significant production of propylene with high selectivities (>70%) and appreciable "initial" steady conversions of propane ranging from *ca*. 27% to 37% at 3 h on-stream. The "initial" steady conversions of propane on the In–Al mixed oxide catalysts decreased in the order: In–Al-20 > In–Al-10 > In–Al-40, pointing to a marked composition effect on the catalytic performance of the In_2O_3–Al_2O_3 samples. From 3 to 8 h, all catalysts underwent noticeable deactivation which could be attributed to carbon deposition on the surface of In_2O_3-based materials, as confirmed by the TG analysis (Table 2). After 8 h on-stream operation, there has been marginal decrease in the conversion of propane with time-on-stream over all mixed oxide catalysts.

Another interesting observation from the time-on-stream tests is that, even after 20 h on-stream operation (Fig. 2), a high conversion of propane up to 26.5% could still be maintained for In–Al-20. It is important to remark that this corresponds to only a 2.9% loss of its quasi steady activity at 8 h on-stream. This is in sharp contrast to the previously reported supported Ga_2O_3-based system for propane dehydrogenation in the presence of CO_2, in which most of the gallia catalysts inclined to deactivate drastically in a few hours [19,25,26]. Indeed, a clear advantage of the In–Al-20 catalyst over a Ga_2O_3 sample was noticed when propane was dehydrogenated using β-Ga_2O_3 under otherwise identical conditions (see Fig. 2). With high selectivity to propylene, such outstanding stability as to the indium-containing catalysts has never been reported before. It is important to note that the slow deactivation of the In–Al-20 sample, when compared to the Ga_2O_3-based catalysts, could be due to the apparently low carbon deposition (see Table 2) as a consequence of its moderate surface acidity [35].

Also presented in Table 1 are the catalytic data of In–Al-20 in the absence of CO_2. The activity of the In–Al-20 catalyst in the presence of CO_2 was twice that in the absence of CO_2. The positive

Table 1
Activity data of the mixed In_2O_3–Al_2O_3 oxide samples.

Sample	Conversion C_3H_8[a] (%)	Yield C_3H_6[a] (%)	Selectivity[a] (%)			
			C_3H_6	CH_4	C_2H_4	C_2H_6
In_2O_3	2.5 (0.4)	1.4 (0.2)	56.0 (56.1)	19.6 (18.5)	17.5 (17.7)	6.9 (7.7)
In–Al-40	27.6 (23.5)	21.9 (19.4)	69.3 (72.7)	17.5 (15.5)	7.6 (6.3)	5.6 (5.5)
In–Al-20	35.7 (29.4)	27.3 (22.8)	76.5 (77.5)	10.2 (10.9)	7.1 (6.6)	6.2 (5.0)
In–Al-10	31.5 (27.2)	23.9 (21.3)	75.8 (78.2)	11.7 (11.1)	7.4 (6.3)	5.1 (4.4)
Al_2O_3	2.5 (0.8)	2.1 (0.7)	85.4 (87.2)	7.1 (6.3)	4.5 (4.1)	3.0 (2.4)
In–Al-20 without CO_2	17.9 (15.1)	14.7 (12.1)	82.0 (80.3)	12.9 (14.1)	2.8 (2.9)	2.3 (2.7)

[a] The value outside and inside the bracket are the data obtained at 3 and 8 h respectively.

Table 2
Physicochemical properties and characterization results of the mixed In_2O_3–Al_2O_3 oxides.

Sample	S_{BET} ($m^2 g^{-1}$)	Coke[a] (%)	In/Al molar ratio		Peak temperature (K)		H_2 consumption (mmol g^{-1})		Percentage of In_2O_3 (α)[f] (%)
			Bulk[b]	Surface[c]	α[d]	β[e]	α[d]	β[e]	
In_2O_3	23	1.5	–	–	–	1026	0	10.3	0
In–Al-40	94	3.8	0.67	0.72	566	980	0. 6	6.0	9.1
In–Al-20	174	5.3	0.25	0.27	573	976	1.6	3.2	33
In–Al-10	195	4.6	0.11	0.13	578	963	1.2	1.4	46
Al_2O_3	233	1.2	–	–	–	–	–	–	–
β-Ga_2O_3	40	11.7	–	–	–	–	–	–	–

[a] The weight percentage of coke amount after 8 h reaction determined by TG.
[b] The bulk In/Al molar ratio calculated from the ICP data.
[c] The surface In/Al molar ratio based on XPS analysis.
[d] The hydrogen consumption during 423–773 K calculated from the TPR results.
[e] The hydrogen consumption during 773–1073 K calculated from the TPR results.
[f] The percentage of In_2O_3 reduced during 423–773 K in TPR from the total amount of In_2O_3 reduced during the whole temperature range.

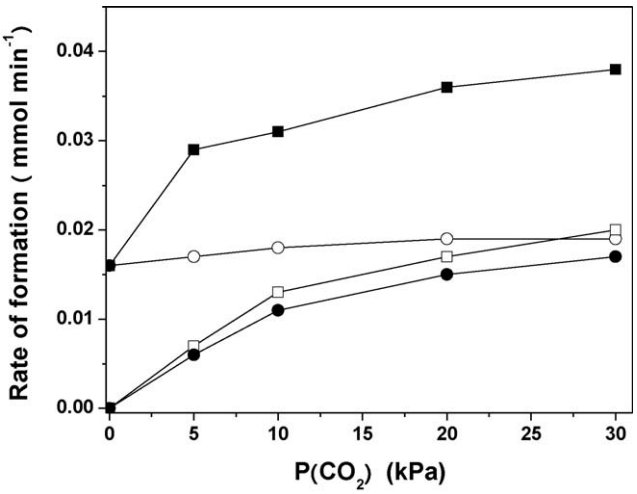

Fig. 3. Dehydrogenation of propane with CO_2 over In–Al-20. Rate of formation: (■) C_3H_6; (○) H_2; (□) CO; (●) H_2O. Reaction conditions: catalyst weight: 200 mg; $P(C_3H_8)$ = 2.5 kPa; $P(N_2)$ = 87.5 kPa; reaction temperature: 873 K; total flow rate: 10 mL min^{-1}.

effect of CO_2 concentration on the propane dehydrogenation over In–Al-20 can be further seen from Fig. 3. All data were collected at the reaction time of 3 h. One can see that the rate of propylene formation remarkably increased together with that of CO and H_2O formation with increasing the partial pressure of CO_2. On the other hand, the rate of H_2 formation showed no significant increase even with increasing the partial pressure of CO_2. All these facts indicate that the essential role of CO_2 is to facilitate the dehydrogenation process ($CH_3CH_2CH_3 \rightarrow CH_2{=}CHCH_3 + H_2$) by reaction of CO_2 with H_2 ($CO_2 + H_2 \rightarrow CO + H_2O$), which shifts the dehydrogenation equilibrium by producing CO and H_2O.

The effect of the reaction temperature on the dehydrogenation activity of the In–Al-20 sample was also examined. Propane conversion and product selectivity as a function of reaction temperature are shown in Fig. 4. With increase of the reaction temperature, propane conversion markedly increased from 8.1% at 773 K to 35.7% at 873 K, whereas the selectivity to propylene decreased from 86.2% at 773 K to 76.3% at 873 K, but the selectivities were still over 75% at temperatures lower than 873 K. Further increase of reaction temperature to 923 K, the conversion has been increased to 48.5%, but the selectivity of

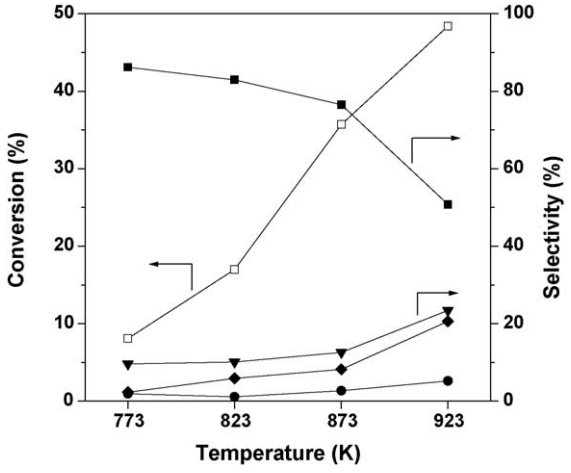

Fig. 4. Effect of reaction temperature on dehydrogenation of propane over In–Al-20; (■) selectivity to propylene; (◇) propylene (△) methane (▼) ethylene (●) ethane yield. Reaction conditions: catalyst weight: 200 mg; $P(C_3H_8)$ = 2.5 kPa; $P(CO_2)$ = 10 kPa; $P(N_2)$ = 87.5 kPa; total flow rate: 10 mL min^{-1}.

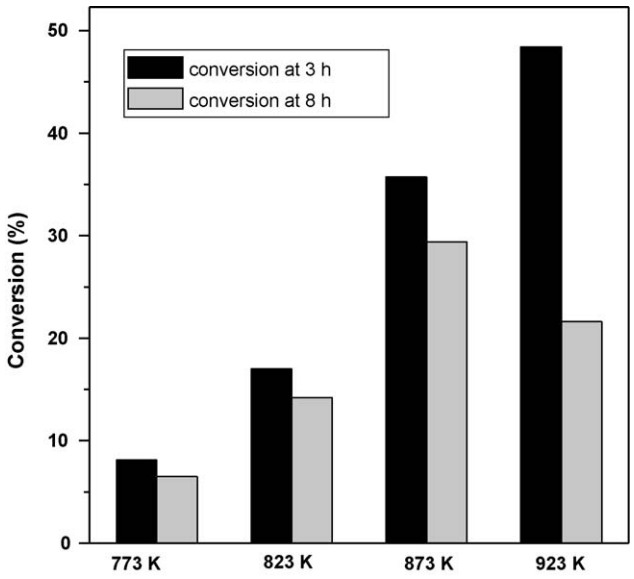

Fig. 5. Conversion of propane for In–Al-20 at different temperatures after the reaction time of 3 and 8 h. Reaction conditions––catalyst weight: 200 mg; $P(C_3H_8)$ = 2.5 kPa; $P(CO_2)$ = 10 kPa; $P(N_2)$ = 87.5 kPa; total flow rate: 10 mL min^{-1}.

propylene has been substantially diminished. Hence, the optimal reaction temperature is 873 K in terms of the maximum yield for propylene production.

The rate of deactivation of the In–Al-20 catalyst increases with increasing the reaction temperature and time as shown in Fig. 5. The rapid deactivation of In–Al-20 was observed at 923 K. After the reaction period of 8 h, the propane conversion dramatically decreased from the "initial" value of 48.5% (activity at 3 h on-stream) to 21.6%. The change in propane conversion was much lower at 873 K; after 8 h the loss of propane conversion amounted to <6.5%. These results clearly indicate that high temperature accelerates coke deposition on the In_2O_3–Al_2O_3 catalyst surface which is extremely detrimental for the maintenance of catalytic stability.

3.2. Catalysts characterization

Fig. 6 illustrates the diffractograms obtained for various In_2O_3–MO_x mixed oxides, along with that of bulk In_2O_3 as a reference. For the sake of convenience, only the representative XRD patterns of for In–Zn-20, In–Si-20, In–Mg-20 and In–Al mixed oxide samples are presented. The bulk In_2O_3 presents a well crystallized phase. The peak intensities and their 2θ angles have been identified as characteristic of the cubic structure of In_2O_3 (*c*-In_2O_3, JCPDS 6-0416). For all mixed oxide samples, except in the case of the In–Al-10 sample, the diffraction peaks corresponding to *c*-In_2O_3 crystalline phase were observed. Note that the diffraction peaks corresponding to crystalline indium oxide phase of all In_2O_3–Al_2O_3 samples are much weaker and broader than those of In–Zn-20, In–Si-20 and In–Mg-20, pointing to apparently higher component dispersion of the In_2O_3–Al_2O_3 composites with respect to the other In-containing mixed oxide materials. Moreover, a progressive attenuation of the diffraction intensity of the crystalline indium oxide phase is observed for the In_2O_3–Al_2O_3 samples with increasing aluminum content. Of particular note is the totally amorphous nature of the In–Al-10 sample, which suggests the highly dispersed nature of the In species in this sample. This was also expected as a result of the highest specific surface area (195 m^2 g^{-1}, see Table 2) of In–Al-10 as compared to other In_2O_3–Al_2O_3 samples.

The redox behavior of the In_2O_3–Al_2O_3 materials has been studied by TPR. As shown in Fig. 7 and Table 2, the TPR profile of

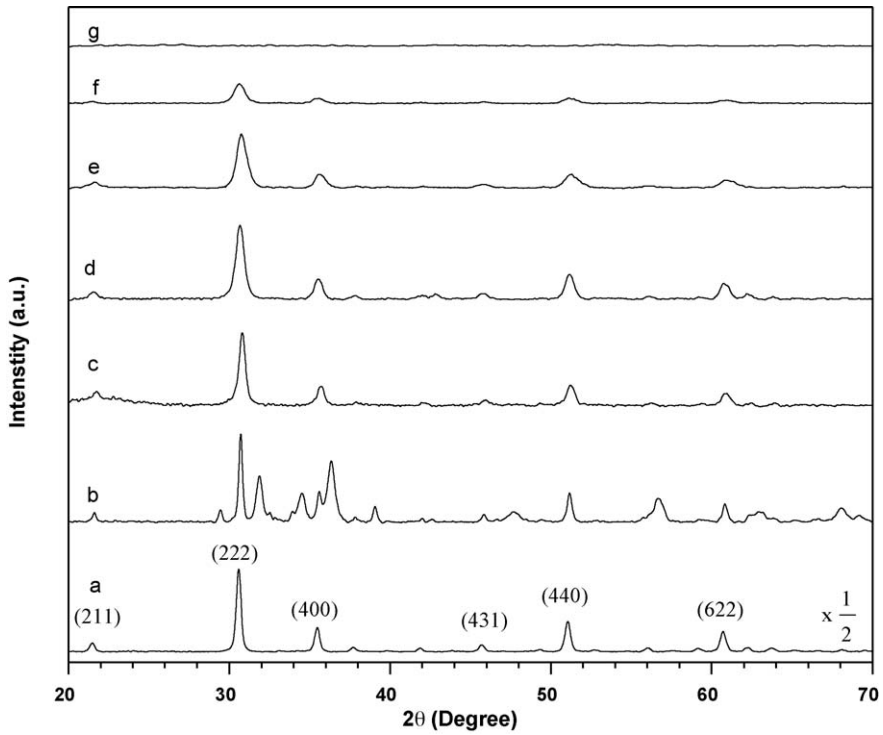

Fig. 6. XRD proffiles for the various In_2O_3–Al_2O_3 mixed oxides: (a) In_2O_3, (b) In–Zn-20, (c) In–Si-20, (d) In–Mg-20, (e) In–Al-40, (f) In–Al-20, and (g) In–Al-10.

bulk In_2O_3 exhibits a single and broad peak centered at 1000 K, attributable to the characteristic reduction of crystalline In_2O_3 to In^0 [28]. The hydrogen consumption is calculated to be 10.3 $mmol_{H2}\ g^{-1}$, corresponding to *ca.* 95% of the complete reduction of indium oxide. Remarkable profiles changes were identified for the reduction of In_2O_3–Al_2O_3 mixed oxide samples, where two distinct reduction features were observed. The main reduction peak (β) ascribed to the reduction of crystalline phase In_2O_3 is shifted to a lower temperature of 963 K in the In–Al mixed oxides, indicative of the presence of a In/Al interaction which facilitates the reduction of the supported In_2O_3 [29]. One can also see that with increasing alumina incorporation, the fraction of low temperature (LT) reduction peak in the temperature range of 473–773 K, attributable to the reduction of dispersed indium oxide phase with smaller particles sizes [29,30], is observed to be the highest for sample In–Al-10 as compared to other In_2O_3–Al_2O_3 samples (Table 2). This observation further confirms the presence of at least two types of In_2O_3 phase in the In_2O_3–Al_2O_3 samples, where crystallized indium oxide (β peak) and In_2O_3 phase highly dispersed on alumina (α peak) co-exist.

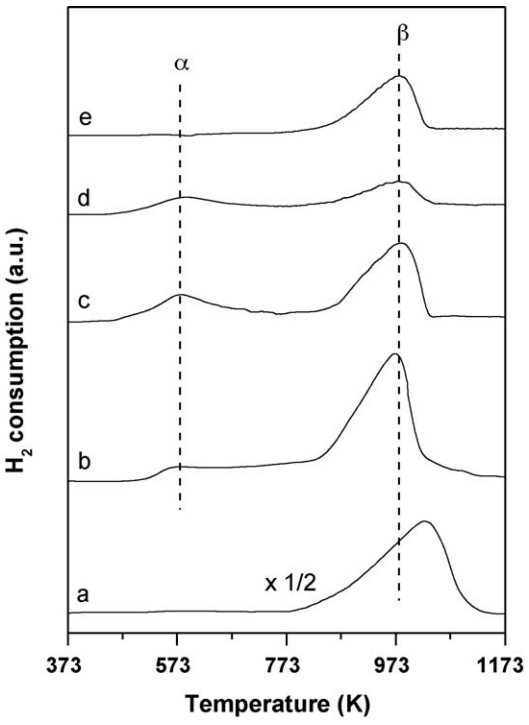

Fig. 7. TPR profiles for the various In_2O_3–Al_2O_3 mixed oxides: (a) In_2O_3, (b) In–Al-40, (c) In–Al-20, (d) In–Al-10, and (e) In–Al-20 reduced by hydrogen at 773 K and subsequently treated by CO_2 at 873 K.

4. Discussion

The main finding reported here is that supported In_2O_3 can be applied as new effective catalyst for the catalytic dehydrogenation of propane to propylene in the presence of CO_2. In_2O_3-containing catalysts, most notably in combination with zeolites and other oxidic materials (e.g. Al_2O_3 or TiO_2) have in the past been shown to exhibit high activity and selectivity in de-NO_x reactions [27–31]. Recently, the high activity and selectivity of In-containing materials in ethanol and methanol steam reforming reactions has also been highlighted [36,37]. In the present work, we have demonstrated that In_2O_3-based binary mixed metal oxide is one of the most effective materials for the dehydrogenation of propane to propylene with CO_2. In this regard, In_2O_3–Al_2O_3 with the optimal 20 mol% indium content was found to be the best catalyst among those studied. More importantly, In_2O_3–Al_2O_3 is shown to be a far better catalyst in terms of catalytic stability for propane DH with CO_2 compared to the most effective Ga_2O_3-based catalysts in the current literature [25,26]. These findings constitute a new basis for the design and development of new catalytic system that exhibits

improved stability and activity for propane dehydrogenation with CO_2.

In view of the interesting catalytic behavior of the In_2O_3-based catalysts, it is of interest to elucidate the likely active species for propane dehydrogenation. It may be noted that no previous studies have employed In-containing materials as catalysts for alkane dehydrogenation. As far as the previously investigated In-catalyzed de-NO_x reactions is concerned, the highly dispersed In_2O_3 species are established to be the active sites for NO_x removal [28–30], in which the reaction occurs via a direct redox mechanism involving alternate reduction and oxidation of the surface In sites. In this context, it may be presumed that the dehydrogenation reaction can proceed via a similar redox mechanism as well. If this holds true, propane is directly oxidized to propylene with a simultaneous reduction of the supported In_2O_3; subsequently, the reduced indium oxide catalyst is reoxidized by CO_2. To confirm this hypothesis, the TPR of the In–Al-20 sample was conducted after "reoxidation" of a H_2-pretreated In–Al-20 sample by CO_2. It should be mentioned, here, that the H_2-pretreatment temperature at 773 K permits the reduction of the highly dispersed In_2O_3 but not the bulk one. As noted above, if the redox pathway is followed, one may expect that the reduced indium species would be readily reoxidized by CO_2 atmosphere at 873 K. Nevertheless, the TPR pattern as shown in Fig. 7e does not show any LT reduction feature in the temperature range of 473–773 K, thus inferring that the direct redox mechanism is probably not applicable for the present In_2O_3-catalyzed dehydrogenation of propane in the presence of CO_2.

To further clarify the active sites in the In_2O_3–Al_2O_3-system, the performance of the most active In–Al-20 catalyst was investigated after the pretreatment with hydrogen (5% H_2/Ar, 673 K and 3 h). It is important to remark that the H_2-pretreatment has a distinct influence on performance evolution of In–Al-20 at the initial stage of the reaction (Fig. 8), with essentially no influence on the steady-state activity of the catalyst for propane dehydrogenation. It is of interest to note that the H_2-pretreated In–Al-20 sample show immediate high initial activity for propane dehydrogenation without experiencing the induction period as observed with the fresh In–Al-20. Meanwhile, it should be pointed out, here, that cracking products (methane and ethylene) are the dominating products in the effluent stream during the induction period (see Fig. 2). Moreover, it is only after the induction period (for *ca.* 3 h on-stream) a steady conversion of propane with pronounced selectivity to propylene can be attained. All these facts, together with the observation that a concomitant reduction of the dispersed In_2O_3 species to corresponding metallic In^0 species has been identified by XPS (not shown), suggests that the induction period during the initial stage of the reaction will transform the as-prepared In_2O_3–Al_2O_3 catalyst to a working catalyst for propylene production.

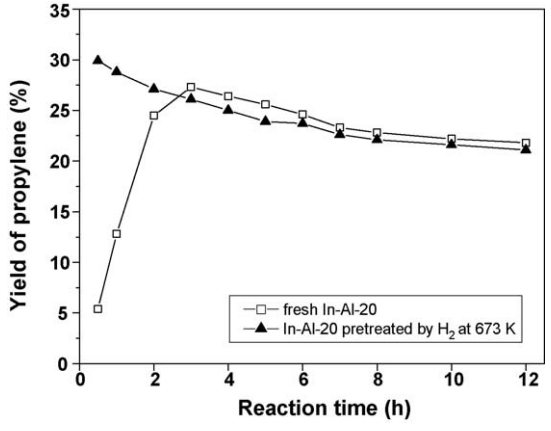

Fig. 8. Yield of propylene as a function of time-on-stream for In–Al-20: (□) fresh sample; (▲) sample that was pretreated by 5 vol% H_2/Ar at 673 K for 3 h; reaction conditions: catalyst weight: 200 mg; $P(C_3H_8)$ = 2.5 kPa; $P(CO_2)$ = 10 kPa; $P(N_2)$ = 87.5 kPa; reaction temperature: 873 K; total flow rate: 10 mL min^{-1}.

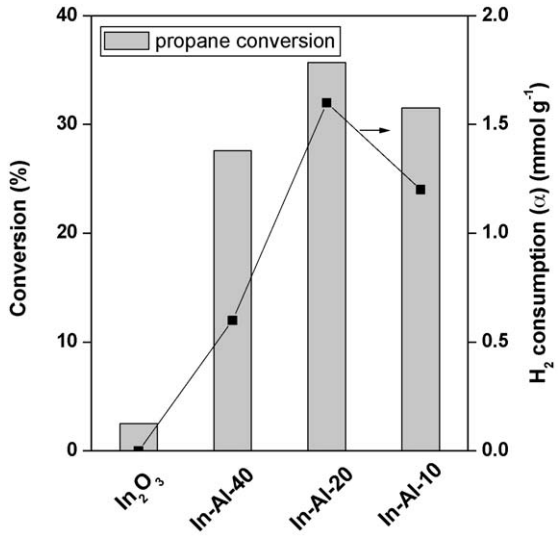

Fig. 9. Relationship between propane conversion at 3 h on-stream and the corresponding hydrogen consumption (α) of the In_2O_3–Al_2O_3 catalysts.

While further work is needed to fully understand the precise nature and mechanism of the surface indium site-mediated hydrocarbon activation, the surface stabilized metallic In^0 nanoclusters that are generated in situ during the induction period could be the key active species for propane dehydrogenation. At this juncture, it is important to highlight that the present In-catalyzed propane dehydrogenation may proceed via a simple dehydrogenation pathway, more specifically the direct propane dehydrogenation mediated by the surface stabilized metallic In^0 species. On the basis of the proposed main reaction pathway as described above, we can rationalize that the surface stabilized metallic In^0 species are the true active sites for propane dehydrogenation. In this context, the favorable in situ creation of In^0 sites from well-dispersed surface indium sites in the mixed oxide catalysts is the key factor in determining the catalytic performance of the In_2O_3–Al_2O_3 materials. This is further supported by the excellent correlation as identified for the relationship (Fig. 9) between the catalytic propane dehydrogenation activity and the amount of In^0 derived from highly dispersed indium species in the present In_2O_3–Al_2O_3 catalysts.

5. Conclusions

This study demonstrates that supported In_2O_3-based materials are new attractive catalysts applicable for propane dehydrogenation with CO_2. Among the various catalysts studied, the In–Al mixed oxides have been found to exhibit superior performance for propane dehydrogenation due to the formation of highly dispersed InO_x species in the as-synthesized materials. Combined XRD and H_2-TPR results demonstrated that the specific interaction between In_2O_3 and Al_2O_3 can result in the formation of In_2O_3–Al_2O_3 in which the structural and surface redox properties are substantially modified. Compared to bulk In_2O_3, the as-prepared In_2O_3–Al_2O_3 mixed oxide catalysts show dramatically enhanced activity for propane dehydrogenation. Our results show that the highest catalytic performance can be attained at a In_2O_3–Al_2O_3 mixed oxide catalyst with a 20 mol% indium content, which allows the steady formation of a maximum propylene yield of *ca.* 27% in the catalytic dehydrogenation of propane at 873 K. The high catalytic

activity of the present In_2O_3–Al_2O_3 catalysts has been attributed to the favorable creation of surface stabilized metallic In^0 nanoclusters as a consequence of in situ reduction of well-dispersed surface indium sites during the induction period.

Acknowledgments

This work was financially supported by the National Natural Science Foundation of China (20633030, 20721063, 20803012, and 20873026), and the National Basic Research Program of China (2009CB623506) and Science & Technology Commission of Shanghai Municipality (08DZ2270500).

References

[1] T. Davies, S.H. Taylor, Catal. Lett. 93 (2004) 151–154.
[2] P. Michorczyk, J. Ogonowski, Appl. Catal. A: Gen. 251 (2003) 425–433.
[3] M. Saito, S. Watanabe, I. Takahara, M. Inaba, K. Murata, Catal. Lett. 89 (2003) 213–217.
[4] S. Sugiyama, Y. Hirata, K. Nakagawa, K.I. Sotowa, K. Maehara, Y. Himeno, W. Ninomiya, J. Catal. 260 (2008) 157–163.
[5] R. Grabowski, Catal. Rev. 48 (2006) 199–268.
[6] D. Vitry, J.-L. Dubois, W. Ueda, J. Mol. Catal. A: Chem. 220 (2004) 67–76.
[7] M.M. Bettahar, G. Costentin, L. Savary, J.C. Lavalley, Appl. Catal. A: Gen. 145 (1996) 1–48.
[8] Y.M. Liu, Y. Cao, K.K. Zhu, S.R. Yan, W.L. Dai, H.Y. He, K.N. Fan, Chem. Commun. (2002) 2832–2833.
[9] Y.M. Liu, Y. Cao, N. Yi, W.L. Feng, W.L. Dai, S.R. Yan, H.Y. He, K.N. Fan, J. Catal. 224 (2004) 417–428.
[10] Y.M. Liu, W.L. Feng, T.C. Li, H.Y. He, W.L. Dai, W. Huang, Y. Cao, K.N. Fan, J. Catal. 239 (2006) 125–136.
[11] K. Takehira, Y. Ohishi, T. Shishido, T. Kawabata, K. Takaki, Q.H. Zhang, Y. Wang, J. Catal. 224 (2004) 404–416.
[12] Y. Sakurai, T. Suzaki, N. Ikenaga, T. Suzuki, Appl. Catal. A: Gen. 192 (2000) 281–288.
[13] H.Y. Li, Y.H. Yue, C.K. Miao, Z.K. Xie, W.M. Hua, Z. Gao, Catal. Commun. 8 (2007) 1317–1322.
[14] Y. Ohishi, T. Kawabata, T. Shishido, K. Takaki, Q.H. Zhang, Y. Wang, K. Takehira, J. Mol. Catal. A: Chem. 230 (2005) 49–58.
[15] Y. Wang, Y. Ohishi, T. Shishido, Q.H. Zhang, W. Yang, Q. Guo, H.L. Wan, K. Takehira, J. Catal. 220 (2003) 347–357.
[16] H. Shimada, T. Akazawa, N. Ikenaga, T. Suzuki, Appl. Catal. A: Gen. 168 (1998) 243–250.
[17] M. Chen, J. Xu, Y.M. Liu, Y. Cao, H.Y. He, J.H. Zhuang, K.N. Fan, Catal. Lett. 124 (2008) 369–375.
[18] M. Chen, J. Xu, F.Z. Su, Y.M. Liu, Y. Cao, H.Y. He, K.N. Fan, J. Catal. 256 (2008) 293–300.
[19] K. Nakagawa, C. Kajita, K. Okumura, N.-o. Ikenaga, M. Nishitani-Gamo, T. Ando, T. Kobayashi, T. Suzuki, J. Catal. 203 (2001) 87–93.
[20] S.B. Wang, Z.H. Zhu, Energy Fuels 18 (2004) 1126–1139.
[21] N. Mimura, I. Takahara, M. Inaba, M. Okamoto, K. Murata, Catal. Commun. 3 (2002) 257–262.
[22] J. Ogonowski, E. Skrzynska, Catal. Lett. 111 (2006) 79–85.
[23] K. Nakagawa, C. Kajita, Y. Ide, M. Okamura, S. Kato, H. Kasuya, N. Ikenaga, T. Kobayashi, T. Suzuki, Catal. Lett. 64 (2000) 215–221.
[24] K. Nakagawa, M. Okamura, N. Ikenaga, T. Suzuki, T. Kobayashi, Chem. Commun. (1998) 1025–1026.
[25] B.J. Xu, B. Zheng, W.M. Hua, Y.H. Yue, Z. Gao, J. Catal. 239 (2006) 470–477.
[26] B. Zheng, W.M. Hua, Y.H. Yue, Z. Gao, J. Catal. 232 (2005) 143–151.
[27] T. Maunula, Y. Kintaichi, M. Haneda, H. Hamada, Catal. Lett. 61 (1999) 121–130.
[28] P.W. Park, C.S. Ragle, C.L. Boyer, M.L. Balmer, M. Engelhard, D. McCready, J. Catal. 210 (2002) 97–105.
[29] J.A. Perdigon-Melon, A. Gervasini, A. Auroux, J. Catal. 234 (2005) 421–430.
[30] A. Gervasini, J.A. Perdigon-Melon, C. Guimon, A. Auroux, J. Phys. Chem. B 110 (2006) 240–249.
[31] M. Haneda, Y. Kintaichi, H. Hamada, Catal. Lett. 55 (1998) 47–55.
[32] M. Takahashi, N. Inoue, T. Nakatani, T. Takeguchi, S. Iwamoto, T. Watanabe, M. Inoue, Appl. Catal. B: Environ. 65 (2006) 142–149.
[33] M. Takahashi, T. Nakatani, S. Iwamoto, T. Watanabe, M. Inoue, Appl. Catal. B: Environ. 70 (2007) 73–79.
[34] K. Shimizu, M. Takamatsu, K. Nishi, H. Yoshida, A. Satsuma, T. Tanaka, S. Yoshida, T. Hattori, J. Phys. Chem. B 103 (1999) 1542–1549.
[35] M. Haneda, E. Joubert, J.C. Menezo, D. Duprez, J. Barbier, N. Bion, M. Daturi, J. Saussey, J.C. Lavalley, H. Hamada, Phys. Chem. Chem. Phys. 3 (2001) 1366–1370.
[36] H. Lorenz, W. Jochum, B. Klotzer, M. Stoger-Pollach, S. Schwarz, K. Pfaller, S. Penner, Appl. Catal. A: Gen. 347 (2008) 34–42.
[37] T. Umegaki, K. Kuratani, Y. Yamada, A. Ueda, N. Kuriyama, T. Kobayashi, Q. Xu, J. Power Sources 179 (2008) 566–570.